An Experimental Intraradicular Biofilm Model in the Pig for Evaluating Irrigation Techniques.

Toshinori Tanaka
Tohoku University
Yoshio Yahata (yahataendo@tohoku.ac.jp)
Tohoku University https://orcid.org/0000-0002-6752-0487
Keisuke Handa
Kanagawa Dental University
Suresh V. Venkataiah
Tohoku University
Mary M. Njuguna
Tohoku University
Masafumi Kahehira
Tohoku University
Tatsuya Hasegawa
Tohoku University
Yuichiro Noiri
Niigata University
Masahiro Saito
Tohoku University

Research article

Keywords: Debridement, intraradicular biofilm model, irrigant activation technique, laser-activated irrigation, pig model, root canal disinfection

Posted Date: October 19th, 2020

DOI: https://doi.org/10.21203/rs.3.rs-92687/v1

Version of Record: A version of this preprint was published at BMC Oral Health on April 7th, 2021. See the published version at https://doi.org/10.1186/s12903-021-01536-w.

Abstract

Background: We established an *in vivo* intraradicular biofilm model of apical periodontitis in pigs in which we compared the efficacy of different irrigant activation techniques for biofilm removal.

Methods: Twenty roots from the deciduous mandibular second premolar of 5 male pigs were used. After pulpectomy, canals were left open for 2 weeks and then sealed for 4 weeks to enable the development of an intracanal biofilm. The intraradicular biofilms was evaluated using SEM and bacterial 16S rRNA gene-sequencing. To investigate the efficacy of biofilm removal, root canal irrigations were performed using conventional needle, passive ultrasonic, subsonic, or laser-activated irrigation. Real-time PCR was conducted to quantitate the remaining biofilm components. Statistical analysis was performed using ANOVA followed by a *Tukey kramer* post-hoc test with $\alpha=0.05$.

Results: The pulp exposure model was effective in inducing apical periodontitis and SEM analysis revealed a multi-layer biofilm formation inside the root canal. 16S rRNA sequence analysis identified Firmicutes, Bacteroidetes, and Fusobacteria as the predominant bacterial phyla components, which is similar to the microbiome profile seen in humans. None of the tested irrigation techniques completely eradicated the biofilm components from the root canal, but the subsonic and laser-activated irrigation methods produced the lowest bacterial counts ($p<0.05$).

Conclusions: An experimental intraradicular biofilm model has been successfully established in pigs. Within the limitations of the study, subsonic or laser-activated irrigation demonstrated the best biofilm removal results in the pig system.

Background

Infection and biofilm formation in the root canal system is an important causative factor for apical periodontitis and current treatments aim to eliminate or substantially decrease the bacterial load within this system [1, 2]. Mechanical instrumentation technology has been developed but has produced an insufficient reduction in bacteria due to the complexity of the root canal system [3–5]. Hence, the action of irrigating solutions is required to reduce the bacterial load to a subcritical level that will promote wound healing of the periapical tissue.

Sodium hypochlorite (NaOCl) is the most commonly used root canal irrigant due to its disinfecting capacity, and its ability to disrupt biofilms and dissolve organic tissues [5–7]. Conventional needle irrigation (CNI) is the standard procedure for delivery of an NaOCl solution, but cannot do so to the entire root canal system, particularly the apical third area where air bubbles often become entrapped and develop a vapor lock effect [8, 9] or create an unexchanged irrigant area which becomes a “dead water” zone [10]. Delivering irrigants close to the root canal apex can also cause severe pain and acute inflammation due to the trade-off in extruding these solutions through the extraradicular area, and can sometimes lead to hospitalization due to the high toxicity of NaOCl towards vital tissues [11]. The establishment of an alternative irrigation technique that can efficiently remove the infection source in the

root canal system is thus essential for improving the efficacy and the outcomes of endodontic treatments.

Various irrigant activation techniques have been proposed to improve irrigant distribution through the canal system, and enhance their antibacterial and antibiofilm capacity [12]. Ultrasonics, subsonics and lasers are widely accepted methods of activating irrigants by applying an external mechanical force. Passive ultrasonic irrigation (PUI) utilizes small noncutting files that oscillate freely in the shaped canals via ultrasonic frequencies (25–30 kHz) that activate irrigants through acoustic streaming [13]. Subsonic irrigation also produces a hydrodynamic phenomenon through oscillating movements at frequencies of 1–10 kHz [12]. Although these techniques are more effective than CNI, the delivery and activation of irrigants through the entire root canal system remains challenging. Laser-activated irrigation (LAI) using an Er:YAG laser has been introduced as an alternative modality for activated root canal irrigation as this radiation can uniquely produce transient cavitation in the liquid through the optical breakdown caused by strong absorption of the laser energy [14, 15]. Hence, a pulsed Er:YAG laser evokes significant fluid movement inside the canal causing shock waves in the solution at the point of collapse, and the subsequently induction of acoustic streaming as a secondary cavitation [16–18]. LAI has been shown to be more effective in artificial biofilm reduction than either CNI or PUI [14, 19–22]. In contrast, Christo et al. found no significant differences in the ability of CNI and LAI to disinfect artificial biofilms [23], indicating that the optimal biofilm removal technique is still a point of contention.

The destruction of biofilms is a crucial requirement for reducing the microbial load in the root canal system, particularly in cases of recurrent periapical pathosis where the biofilms are causative for pathogenesis. The microbiota of an infected root canal are typically polymicrobial, and in the case with a mature microbiota, bacteria do not exist as separate colonies or in planktonic form, but as integrated communities attached to the root canal walls as biofilms [24, 25]. These attached biofilms are embedded within a self-produced extracellular polymeric matrix which is resistant to root canal irrigants [26, 27]. Numerous studies have been conducted to evaluate the efficacy of different irrigation protocols in disinfecting biofilms, but these investigations have typically used an *ex vivo* model involving an extracted tooth, an *in vitro* plastic tooth model or computational fluid dynamics. An artificial biofilm model developed using *Enterococcus feacalis*, which is a very relevant species for recurrent periapical pathosis because it is difficult to remove by root canal treatment, has also been developed to evaluate the efficacy of root canal irrigation systems [6, 28]. However, these *ex vivo* and *in vitro* studies have mainly involved monospecies biofilms and were therefore limited in terms of providing insights into removing biofilms that actually form in infected root canals, and can invade the dentinal tubules and strongly bind to the root canal wall.

Mouse and rat experimental models have also been developed to induce biofilm formation inside the root canal system by means of a left open pulp chamber that enabled the ingrowth of oral bacteria [29]. These systems have provided a good understanding of the expansion and inflammation processes and pathways leading to a periapical lesion. Notably however, rodent teeth are too small to test the effectiveness of root canal irrigation. In contrast, the pig is a useful animal model to evaluate the biofilm

removal efficiency of root canal irrigation techniques used in human because of the similar physiologic characteristics and tooth morphologies between pigs and humans [30]. We aimed in our current study to develop an *in vivo* intraradicular biofilm and apical periodontitis model in cattle pigs and use this system to compare the efficacy of biofilm removal between different irrigant activation techniques that can be applied in humans.

Methods

Ethics statement

This study was reviewed and approved by the Animal Care and Use Committees of Tohoku University Graduate school of Dentistry (Permit No. 2017 DnA-024). All animal experiments and procedures were conducted in accordance with the Regulations for Animal Experiments and Related Activities at Tohoku University. Dental interventions were performed under sodium pentobarbital anesthesia and local injections of lidocaine to minimize the animal's suffering.

Induction of periapical bone defect in pigs

The experimental protocols used in our current investigations are outlined in Fig. 1. Five two-month-old male pigs (Large white □ Landrace breed cross) were obtained from Japan SLC Inc. (Shizuoka, Japan). Twenty roots from 10 lower deciduous mandibular second premolars were used in the experiments. In our animal facility, the light is turned on at 8 o'clock and turned off at 18 o'clock. Pigs can freely drink water at any time and eat normal diet (Grandeal B; Zennoh Feed Mills of the Tohoku District, Miyagi, Japan) 3 times every day. All procedures were performed with surgical loupes with LED light (EyeMag PRO; Carl Zeiss, Jena, Germany) under general anesthesia (sevoflurane) and a local anesthetic (2% lidocaine). Briefly, the occlusal surfaces were flattened with a straight bur and electric engine (Ti-Max X95; NSK, Tochigi, Japan) to prevent tooth fracture and for ease of working length determination. Following access cavity preparation and straight-line access with burs, a pulpectomy was performed with 6% sodium hypochlorite and K files. Pulp tissue was then removed and the working length was determined with radiograph (Fig. 1d). After subsequent chemo-mechanical debridement, canals were exposed to the oral environment for 2 weeks, after which coronal openings were sealed with hydraulic temporary filling material (Lumicon; Kulzer Japan, Tokyo, Japan) and composite resin (MI Flow II; GC, Tokyo, Japan) to create an anaerobic intracanal environment for 4 weeks. At 6 weeks after the pulpectomy, the induced periapical bone defects were scanned with a micro-CT device (ScanXmate E090; Comscantecno, Kanagawa, Japan). Six roots of the periapical bone defects were scanned, and the defect volumes were analyzed and quantified using image analysis software (TRI/3D-BON; Ratoc System Engineering, Tokyo, Japan). The lesion area was defined by configuring the boundary radiopaque area including the bone and teeth that surrounded the lesion. The lesion volume was then calculated as the region enclosed by the bounded radiopaque area. Blood samples were taken from 3 pigs prior to the pulpectomy, and at 2 and 6 weeks after this procedure, to determine the inflammation stage via a C-Reactive Protein Assay (CRP).

Irrigation protocol

At 6 weeks after the pulpectomy procedure, the pigs were anesthetized with sevoflurane and local anesthesia prior to undergoing the root canal irrigation. For the control group (n = 4), teeth were extracted and intracanal biofilms were evaluated by SEM observations (n = 1) and real-time PCR (n = 3). The dental calculus was removed prior to treatment using an ultrasonic tip and device (Solfy F; Morita, Kyoto, Japan), and teeth were isolated with a rubber dam clamp (#212; Hu-friedy, Chicago, IL, USA) and rubber dam sheet (KSK Dental Dam Medium; Dentech, Tokyo, Japan). Aseptic conditions were established by cleaning the tooth with 3% hydrogen peroxide and 6% sodium hypochlorite, as described by Ng et al. [31] with some modifications. After temporary filling material removal, tooth were randomly divided into 4 groups for root canal irrigation: conventional 30 gauge close-ended needle irrigation (ProRinse Endo Irrigation Needles; Dentsply Sirona, PA, USA) with 6% sodium hypochlorite (CNI), CNI + ultrasonic activation (Solfy F; Morita) using a #15/02 tip (PUI), CNI + subsonic activation (EndoActivator, Dentsply Sirona) with a #15/02 tip (EA), and CNI + laser activation (LAI) with a 2.94 μm wavelength Er:YAG laser (Erwin AdvErL EVO; Morita). The randomization sequence was created using a computer-generated list using Excel 2016 (Microsoft, Redmond, WA, USA). During root canal irrigation, mechanical instrumentation was not performed.

In the CNI group (n = 4), canals were irrigated for 30 seconds (1 mL) and then left for 30 seconds, which is a procedure modified from the protocol of Al-Jadaa et al. [32]. This cycle was repeated 5 times (total procedure time, 5 minutes). In the PUI group (n = 4), canals were irrigated for 30 seconds (1 mL) with a 30G close-ended needle and irrigants were activated for 30 seconds ultrasonically (ENDO mode; power, 10). This cycle was repeated 5 times (total procedure time, 5 minutes). The EA and LAI methods (n = 4 each) involved the same procedures as PUI but the irrigants were instead activated with EndoActivator (power; high) and using an Er:YAG laser, respectively. For LAI, the activation was operated at 50 mJ of pulse energy, a 20 Hz of frequency, and a 300 μsec of pulse rate. The optic fiber (R300T, Morita) was 14 mm in length from the handpiece with a 300 μm fiber diameter and had a conical tip at the approximately 160 μm from the tip with an 84 degree angle. The tips of irrigation needles, ultrasonic, Endoactivator, and Er:YAG laser were all placed 3 mm short from working length and gently moved back and forth during irrigation and activation.

Following irrigation, each root canal was rinsed with 2 mL saline in total for 30 seconds. The access cavities were then sealed again with composite resin and the pigs were euthanized with a lethal dose of potassium chloride (0.25 mEq/kg, IV) under deep general anesthesia for tooth extraction. Prior to tooth extraction, we performed calculous removal and tooth cleaning to reduce the risk of bacterial contamination. The crowns were removed with a disc bur, and any remaining bacterial infection in each root was evaluated by SEM (n = 1 each) and real-time PCR (n = 3 each) to determine the bacterial count.

Scanning electron microscopy

The crown of each experimental tooth was cut and removed using a diamond disc to separately obtain mesial and distal roots. One distal root from each experimental sample was then observed by SEM.

Briefly, the roots were grooved longitudinally on the outer surface with a diamond disc and then split into two halves with a chisel. The specimens were then fixed with 2.5% glutaraldehyde for more than 24 hours, rinsed with PBS three times, and then treated with 1-ethyl-3-methyl-imidazolumtetrafluoroborate. After absorption of the excess, samples were dried in a vacuum desiccator for 1 day and slightly sputter-coated with platinum. The surfaces of each sample were inspected using a VE-8800 scanning electron microscope (Keyence Inc., Osaka, Japan) at a 10 kV acceleration, and the images were obtained at 30, 1 k, and 5 k magnifications.

Bacterial 16S rRNA gene analysis

The sample pig teeth were extracted from the jaw bone and the tooth crowns were resected and immediately frozen in liquid nitrogen. The roots were then crushed to powder using an SK mill (Tokken, Chiba, Japan). Total DNA was extracted from each powdered root sample using a Cica Geneus DNA extraction Kit (KANTO chemical co.; Tokyo, Japan) in accordance with the manufacturer's instructions.

Bacterial sequencing analysis of the intraradicular biofilms was conducted as described by Reyes et al. [33]. Briefly, the V3-V4 region of 16S rRNA was amplified using 16S (V3-V4) metagenomic library construction kit for NGS (Takara Bio Inc, Shiga, Japan) with the primer pairs for 341F (5'-TCGTCGGCAGCGTCAGATGTGTATAAGAGACAGCCTACGGGNGGCWGCAG-3') and 806R (5'-GTCTCGTGGGCTCGGAGATGTGTATAAGAGACAGGGACTACHVGGGTWTCTAAT-3'). Purification and quantification of the PCR amplicons were performed using Agencourt AMpure magnetic beads (Beckman Coulter, Indianapolis, IN, USA) for subsequent pyrosequencing. Index PCR assays were performed using a Nextera XT index kit (Illumina, San Diego, CA, USA) and the amplicons were again purified with the AMpure magnetic beads. An Illumine Miseq platform (Illumina) was next used to generate 250-bp paired-end sequences which were processed via the QIIME bioinformatic pipeline. After removing low-quality sequences, noise, pyrosequencing errors, and chimeras, the reads were clustered into operational taxonomic units (OTUs) with a 0.97 clustering threshold using the CD-HIT-OTU. To acquire the taxonomic classification for each OTU, representative sequences were aligned to the GreenGens database (gg_13_8) and assigned to this repository using RDP classifier v.2.2. Likewise, a homology search was performed for these sequences for assignment to the DDBJ 16S ribosomal RNA database.

Quantification of bacterial populations in the root canal

Quantifications of the bacteria present in the root canals were performed based on previously described methods [29, 34] using the remaining powdered roots from each experimental sample. The presence of bacteria was verified in the experimental samples by qPCR using the bacterial primers 357F and 908R22. These assays were performed using a real-time PCR apparatus (CFX Connect, Bio-Rad Laboratories, Hercules, CA, USA). Amplifications were conducted for 40 cycles at 95 °C for 15 seconds followed by 65 °C for 1 minute, with the fluorescence signals measured at the end of each cycle. A standard curve was generated by subjecting 10-fold dilutions of a known concentration of *E. faecalis* DNA to the same qPCR protocol. The bacterial counts in all of the experimental groups were calculated using threshold cycle (Ct) values plotted against the standard curve. Statistical analysis was performed using ANOVA,

followed by a *Tukey kramer* post-hoc test using IBM SPSS, version 22 (IBM SPSS Statics, Chicago, IL, USA) with an α value of 0.05, to detect significant differences in the bacterial populations.

Results

Periapical lesion formation in the pig model

Stereomicroscopic views of the dissected mandibular jaws from our intraradicular biofilm model in pigs demonstrated bone defects at the buccal side of the apex (Fig. 2a). Micro-CT analysis in a frontal (Fig. 2b), horizontal (Fig. 2c), sagittal (Fig. 2d), and 3D view (Fig. 2e) revealed periapical lesion formation at both the mesial and distal roots. The mean volume of these periapical bone defects at 6 weeks after pulpectomy was $126.3 \pm 97.3 mm^3$. The mean CRP level was 93 μg/mL prior to the pulpectomy, 147 μg/mL at 2 weeks, and 129 μg/mL at 6 weeks (Fig. 3). The CRP level was not increased significantly, but was higher at 2 weeks and lower at 6 weeks, although still above the 0 week baseline, indicating that inflammation had been induced by the periapical lesion.

Characterization of the intraradicular biofilm in the pig model

Using SEM observations, we found that the root canal wall in our pig model was almost completely covered with debris, extracellular-matrix-like structures, and typical three-dimensional biofilm structures (Fig. 4a). Numerous cocci and some rods were also aggregated in most parts of the root canal wall area (Fig. 4b, c). Bacterial 16S rRNA sequence analysis of the biofilm formations in the root canals of the pigs identified Firmicutes (28.04%), Bacteroidetes (21.69%), and Fusobacteria (19.97%) as the major bacterial phyla, which was significant as these are also the predominant bacterial phyla components in human periapical lesions (Fig. 4d).

Effects of root canal irrigation techniques in the pig model

We investigated the biofilm-cleaning ability of CNI, PUI, EA and LAI in the infected root canals in the pig model. The CNI and PUI groups still had debris attachment on the root canal wall (Fig. 5a, b), whereas EA and LAI resulted in lower debris compared with CNI and PUI (Fig. 5c, d). Higher magnification views revealed that a multi-layered biofilm structure could be seen in the CNI and PUI groups (Fig. 5e, f), whereas the EA and LAI treatments showed fewer remnants of debris (Fig. 5g, h). The root canal surface underwent LAI showed a slight opening of the dentinal tubules compared with the other groups (Fig. 5h). Quantitative PCR analysis further revealed that the number of bacteria in the infected root canal was the most significantly reduced in the LAI group (5.5×10^7 cells) and EA group (6.0×10^7 cells) compared with the PUI group (1.1×10^8 cells) and CNI group (1.4×10^8 cells) (Fig. 6). In contrast, no significant difference were observed between the CNI and control groups (1.7×10^8 cells), whereas the PUI group showed a

lower bacterial number than the control group (Fig. 6). There were no significant differences between CNI and PUI groups, and among sound tooth, LAI and EA groups (*Tukey Kramer* test, $p < 0.05$).

Discussion

Many experimental models and approaches have been employed to date to evaluate the efficacy of root canal irrigation. Classically, radiopaque irrigants *in vivo* or dye solutions used in transparent root canal models *in vitro* have been utilized to monitor the penetration of these solutions [35–42]. Artificially placed dentine debris using a split tooth is a simple method of determining the influence of irrigation and irrigant activation techniques by scoring the remaining debris [43, 44]. Organic tissues have also been used to evaluate chemical debridement and the efficacy of irrigant activation, and it has been revealed that ultrasonic activation enhances chemical debridement in simulated curved canals and accessory canals [32, 45]. Computational fluid dynamics (CFD) has also provided a further understanding of fluid flow mechanisms [10, 46–49]. CFD studies have provided measurements of velocity magnitude, velocity vectors, and wall shear stresses with various needle designs and positioning. The effects of various irrigating solutions against endodontic biofilm have been assessed in previous reports, particularly from a chemical aspect, and optimal irrigant concentrations and temperatures have been described [26, 50–53]. Notably however, no *in vivo* study models had yet been developed to compare the efficacy of different irrigation protocols for clinical biofilm removal [54].

Pigs have been adopted as an experimental model in many biomedical fields due to some clear similarities with the human anatomy, and due to the obvious ethical considerations with regard to human subjects. Alveolar bone mineral contents, and the inflammation and destruction processes in periodontal tissues, are among the notable biological similarities between pigs and humans [30, 55]. In our current experimental pig model, we could successfully observe bone defects at the periapical area after exposing the root canal system to the oral environment. These defects developed as a consequence of inflammation, confirmed by an increased CRP level at 2 weeks after root canal exposure. As found in previous studies, intraradicular biofilms can arise through the opening of an access cavity for 2 weeks to enable contamination, and subsequent sealing for 4 weeks to produce an anaerobic environment [56, 57]. We observed typical biofilm thickness in the entire root canals in our pig model by SEM imagery in the control tooth. Importantly, we confirmed in our current experimental pig model that the most abundant and prevalent phyla within the intracanal biofilms were Firmicutes, Bacteroidetes and Fusobacteria, which predominate also in human samples [58]. Although, we did not use controls for bacterial 16S rRNA gene analysis, the results are comparable to the previously reported human data based on the robust experimental protocols for the gene analysis [33, 59, 60]. In our current study in the pig, we utilized the lower deciduous mandibular second premolars because this tooth length is similar to that in humans. Although the apical size of approximately 0.7-1.0 mm in diameter is wider, and the root dentin thickness is thinner, in the pig than in human permanent teeth, the same armamentarium used for root canal treatments in human clinical practice can be readily applied also in a pig model. The intraradicular biofilm pig model is therefore far more reflective of human conditions than those created using rodents or rabbits.

We focused in our present study on the chemical reduction of biofilm using NaOCl [61] and agitating irrigation techniques. Hence, we did not utilize mechanical instrumentation nor EDTA irrigation. Mechanical instrumentation is absolutely essential for the mechanical debridement of biofilm and to reduce the bacterial count from the root canal. Mechanical debridement may be sufficient in an experimental system for reducing biofilm if the tooth has a straight and wide i.e. although mechanical instrumentation is essential, it has an inherent limitation for the complete shaping of the root canal system. To eradicate biofilm from these unreached areas, root canal irrigation, in which the irrigant is agitated using a physical reaction, is likely to be needed. A notable limitation of our current study however was that the tooth did not represent a curved canal. Future studies should consider comparing the efficacy of different techniques for the *in vivo* removal of an intraradicular biofilm from a curved root canal.

We used our pig model system to test the effectiveness of various established human irrigation protocols in removing biofilm from the root canal system. In terms of bacterial quantification however, it must be pointed out that the actual oral hygiene of pig is a poor. Thus, although calculous removal and tooth cleaning were performed in our pigs before extraction to reduce bacterial contamination, the sound tooth was served as a control for quantification analysis. Hence, although contamination by bacteria may occur during tooth extraction in a pig model system, our results showed that all of the tooth samples with induced biofilm formation had a significantly higher number of bacteria than the sound tooth. In accordance with previous reports, the CNI method was found in our current analysis to be insufficient to clean the root canals due to its delivery limitations [62, 63]. Our findings indicated in fact that almost no biofilm was removed by CNI. A large number of prior PUI studies have reported positive results in the removal of intracanal hard tissue debris and pulp tissue remnants due to the acoustic streaming generated by oscillating movements [12, 64, 65]. However, PUI was further found to be less effective than chemo-mechanical preparation in a large canal [28], indicating that it is limited in terms of intraradicular biofilm removal from a wide root canal. Our current results in the pig model were consistent with this as we found no significant differences between the efficacy of CNI and PUI.

The subsonic energy in the EA method has been found to generate a higher back-and-forth tip movement amplitude. The effectiveness of EA in cleaning an infected root canal and in smear layer removal is reported to be inferior or equal to that of PUI [66–68]. The main difference between EA and PUI is whether the tip of the device directly contacts the root canal surface or not. The range of the vibrating polymer tip of the EA is much wider than the range of motion of a PUI tip, and this increases the area where the tip makes physical contact with the root canal surface. Hence, our current results with EA in the pig model suggest that the generation of a mechanical force against the root canal wall is essential for eliminating firmly attached biofilms.

LAI produces a physical reaction in the irrigant solution by transient cavitation through the optical breakdown caused by the strong absorption of the laser energy, which is expected to remove biofilm [69]. Our current findings in the pig model indicate that LAI is more effective at removing intraradicular biofilms than CNI or PUI, which is consistent with previous *in vitro* studies [21, 22]. Hence, the adjunctive

mechanical reaction is attributable to the highly turbulent action of the irritant, and the photo-initiated energy is effective in collapsing the intraradicular biofilms. These results also suggested the further potential of LAI, which generates a mechanical reaction without contacting the root canal wall and can have effects beyond the root canal curvature or irregular areas such as isthmus, fin, and accessory canals. Further studies are needed to investigate whether such mechanical turbulence in irrigants generated by LAI can penetrate sufficiently to produce the shear stress required to remove biofilms.

Conclusions

An experimental intraradicular biofilm model has been successfully established in the pig. Analyses using this model strongly suggested that agitating root canal irrigants with sufficient physical reaction stress at the root canal wall is important to disrupt and remove the biofilm within the root canal. Our novel *in vivo* biofilm model in the pig will likely make important future contributions to improving the efficacy of root canal treatment.

Abbreviations

NaOCl: Sodium hypochlorite; CNI: Conventional needle irrigation; LAI: Laser-activated irrigation; CRP: C-reactive protein assay; PUI: Passive ultrasonic irrigation; EA: EndoActivator; OTUs: Operational taxonomic units; CFD: Computational fluid dynamics

Declarations

Ethical approval and consent to participate

This study was reviewed and approved by the Animal Care and Use Committees of Tohoku University Graduate school of Dentistry (Permit No. 2017 DnA-024). All applicable international, national, and/or institutional guidelines for the care and use of animals were followed. Consent to participate was not applicable.

Consent for publication

Not applicable.

Availability of data and materials

All the datasets used and analyzed during the current study are available from the corresponding author on reasonable request.

Competing interest

The authors declare that they have no competing interest.

Funding

This work was supported by a Grant-in-Aid for Scientific Research (C) from the Japan Society for Promotion of Science (Grant Number 18K09592). The funding source had no role in any part of the research process.

Authors' contribution

TT and YY developed the conception and design of this study. TT, YY and KH acquired the experimental data. SVV, MMN, MK and HT contributed to analysis and interpretation of data. TT and YY drafted the manuscript. TT, YY, YN and MS revised the manuscript. All authors read and approved the final manuscript.

Acknowledgements

We are extremely grateful to Dr. Taiji Nagahashi for his valuable advice and discussions during the course of this work, and Ms. Teruko Sueta for assistance with the animal experiments.

Author details

[1]Division of Operative Dentistry, Department of Ecological Dentistry, Tohoku University Graduate School of Dentistry, Miyagi, Japan

[2]Division of Molecular Biology and Oral Biochemistry, Department of Oral Science, Graduate School of Dentistry, Kanagawa Dental University, Kanagawa, Japan

[3]Division of Cariology, Operative Dentistry and Endodontics, Department of Oral Health Science, Niigata University Graduate School of Medical and Dental Sciences, Niigata, Japan

References

1. Kakehashi S, Stanley HR and Fitzgerald RJ. The effects of surgical exposures of dental pulps in germ-free and conventional laboratory rats. Oral Surg Oral Med Oral Pathol. 1965;20:340-9.
2. Moller AJ, Fabricius L, Dahlen G, Ohman AE and Heyden G. Influence on periapical tissues of indigenous oral bacteria and necrotic pulp tissue in monkeys. Scand J Dent Res. 1981;89:475-84.
3. Peters OA, Schonenberger K and Laib A. Effects of four Ni-Ti preparation techniques on root canal geometry assessed by micro computed tomography. Int Endod J. 2001;34:221-30.

4. Peters OA, Peters CI, Schonenberger K and Barbakow F. ProTaper rotary root canal preparation: effects of canal anatomy on final shape analysed by micro CT. Int Endod J. 2003;36:86-92.
5. Dutner J, Mines P and Anderson A. Irrigation trends among American Association of Endodontists members: a web-based survey. J Endod. 2012;38:37-40.
6. Mohmmed SA, Vianna ME, Penny MR, Hilton ST and Knowles JC. The effect of sodium hypochlorite concentration and irrigation needle extension on biofilm removal from a simulated root canal model. Aust Endod J. 2017;43:102-109.
7. Naenni N, Thoma K and Zehnder M. Soft tissue dissolution capacity of currently used and potential endodontic irrigants. J Endod. 2004;30:785-7.
8. Ram Z (1977) Effectiveness of root canal irrigation. Oral Surg Oral med Oral Path. 1977;44:306-12.
9. Versiani MA, De-Deus G, Vera J, Souza E, Steier L, Pecora JD and Sousa-Neto MD. 3D mapping of the irrigated areas of the root canal space using micro-computed tomography. Clin Oral Investig. 2015;19:859-66.
10. Gao Y, Haapasalo M, Shen Y, Wu H, Li B, Ruse ND and Zhou X. Development and validation of a three-dimensional computational fluid dynamics model of root canal irrigation. J Endod. 2009;35:1282-7.
11. Guivarc'h M, Ordioni U, Ahmed HM, Cohen S, Catherine JH and Bukiet F. Sodium hypochlorite accident: a systematic review. J Endod. 2017;43:16-24.
12. Gu LS, Kim JR, Ling J, Choi KK, Pashley DH and Tay FR. Review of contemporary irrigant agitation techniques and devices. J Endod. 2009;35:791-804.
13. van der Sluis LW, Versluis M, Wu MK and Wesselink PR. Passive ultrasonic irrigation of the root canal: a review of the literature. Int Endod J. 2007;40:415-26.
14. De Moor RJ, Blanken J, Meire M and Verdaasdonk R. Laser induced explosive vapor and cavitation resulting in effective irrigation of the root canal. Part 2: evaluation of the efficacy. Lasers Surg Med. 2009;41:520-3.
15. Meire MA, Poelman D and De Moor RJ. Optical properties of root canal irrigants in the 300-3,000-nm wavelength region. Lasers Med Sci. 2014;29:1557-62.
16. Blanken J, De Moor RJ, Meire M and Verdaasdonk R. Laser induced explosive vapor and cavitation resulting in effective irrigation of the root canal. Part 1: a visualization study. Lasers Surg Med. 2009;41:514-9.
17. Matsumoto H, Yoshimine Y and Akamine A. Visualization of irrigant flow and cavitation induced by Er:YAG laser within a root canal model. J Endod. 2011;37:839-43.
18. Gregorcic P, Jezersek M and Mozina J. Optodynamic energy-conversion efficiency during an Er:YAG-laser-pulse delivery into a liquid through different fiber-tip geometries. J Biomed Opt. 2012;17:075006.
19. De Moor RJ, Meire M, Goharkhay K, Moritz A and Vanobbergen J. Efficacy of ultrasonic versus laser-activated irrigation to remove artificially placed dentin debris plugs. J Endod. 2010;36:1580-3.

20. de Groot SD, Verhaagen B, Versluis M, Wu MK, Wesselink PR and van der Sluis LW. Laser-activated irrigation within root canals: cleaning efficacy and flow visualization. Int Endod J. 2009;42:1077-83.
21. Peters OA, Bardsley S, Fong J, Pandher G and Divito E. Disinfection of root canals with photon-initiated photoacoustic streaming. J Endod. 2011;37:1008-12.
22. Ordinola-Zapata R, Bramante CM, Aprecio RM, Handysides R and Jaramillo DE. Biofilm removal by 6% sodium hypochlorite activated by different irrigation techniques. Int Endod J. 2014;47:659-66.
23. Christo JE, Zilm PS, Sullivan T and Cathro PR. Efficacy of low concentrations of sodium hypochlorite and low-powered Er,Cr:YSGG laser activated irrigation against an Enterococcus faecalis biofilm. Int Endod J. 2016;49:279-86.
24. Ricucci D and Siqueira JF, Jr. Biofilms and apical periodontitis: study of prevalence and association with clinical and histopathologic findings. J Endod. 2010;36:1277-88.
25. Nair PN, Sjogren U, Krey G, Kahnberg KE and Sundqvist G. Intraradicular bacteria and fungi in root-filled, asymptomatic human teeth with therapy-resistant periapical lesions: a long-term light and electron microscopic follow-up study. J Endod. 1990;16:580-8.
26. Wang Z, Shen Y and Haapasalo M. Effectiveness of endodontic disinfecting solutions against young and old Enterococcus faecalis biofilms in dentin canals. J Endod. 2012;38:1376-9.
27. Clegg MS, Vertucci FJ, Walker C, Belanger M and Britto LR. The effect of exposure to irrigant solutions on apical dentin biofilms in vitro. J Endod. 2006;32:434-7.
28. Pladisai P, Ampornaramveth RS and Chivatxaranukul P. Effectiveness of different disinfection protocols on the reduction of bacteria in Enterococcus faecalis biofilm in teeth with large root canals. J Endod. 2016;42:460-4.
29. Yoneda N, Noiri Y, Matsui S, Kuremoto K, Maezono H, Ishimoto T, Nakano T, Ebisu S and Hayashi M. Development of a root canal treatment model in the rat. Sci Rep. 2017;7:3315.
30. Wang S, Liu Y, Fang D and Shi S. The miniature pig: a useful large animal model for dental and orofacial research. Oral Dis. 2007;13:530-7.
31. Ng YL, Spratt D, Sriskantharajah S and Gulabivala K. Evaluation of protocols for field decontamination before bacterial sampling of root canals for contemporary microbiology techniques. J Endod. 2003;29:317-20.
32. Al-Jadaa A, Paque F, Attin T and Zehnder M. Acoustic hypochlorite activation in simulated curved canals. J Endod. 2009;35:1408-11.
33. Reyes A, Haynes M, Hanson N, Angly FE, Heath AC, Rohwer F and Gordon JI. Viruses in the faecal microbiota of monozygotic twins and their mothers. Nature. 2010;466:334-8.
34. Kuremoto K, Noiri Y, Ishimoto T, Yoneda N, Yamamoto R, Maezono H, Nakano T, Hayashi M and Ebisu S. Promotion of endodontic lesions in rats by a novel extraradicular biofilm model using obturation materials. Appl Environ Microbiol. 2014;80:3804-10.
35. Salzgeber RM and Brilliant JD. An in vivo evaluation of the penetration of an irrigating solution in root canals. J Endod. 1977;3:394-8.

36. Abou-Rass M and Piccinino MV. The effectiveness of four clinical irrigation methods on the removal of root canal debris. Oral Surg Oral Med Oral Pathol. 1982;54:323-8.
37. Chow TW. Mechanical effectiveness of root canal irrigation. J Endod. 1983;9:475-9.
38. Kahn FH, Rosenberg PA and Gliksberg J. An in vitro evaluation of the irrigating characteristics of ultrasonic and subsonic handpieces and irrigating needles and probes. J Endod. 1995;21:277-80.
39. Zehnder M. Root canal irrigants. J Endod. 2006;32:389-98.
40. de Gregorio C, Estevez R, Cisneros R, Paranjpe A and Cohenca N. Efficacy of different irrigation and activation systems on the penetration of sodium hypochlorite into simulated lateral canals and up to working length: an in vitro study. J Endod. 2010;36:1216-21.
41. Tay FR, Gu LS, Schoeffel GJ, Wimmer C, Susin L, Zhang K, Arun SN, Kim J, Looney SW and Pashley DH. Effect of vapor lock on root canal debridement by using a side-vented needle for positive-pressure irrigant delivery. J Endod. 2010;36:745-50.
42. Vera J, Hernandez EM, Romero M, Arias A and van der Sluis LW. Effect of maintaining apical patency on irrigant penetration into the apical two millimeters of large root canals: an in vivo study. J Enodod. 2012;38:1340-3.
43. van der Sluis LW, Gambarini G, Wu MK and Wesselink PR. The influence of volume, type of irrigant and flushing method on removing artificially placed dentine debris from the apical root canal during passive ultrasonic irrigation. Int Endod J. 2006;39:472-6.
44. Jiang LM, Verhaagen B, Versluis M and van der Sluis LW. Evaluation of a sonic device designed to activate irrigant in the root canal. J Endod. 2010;36:143-6.
45. Al-Jadaa A, Paque F, Attin T and Zehnder M. Necrotic pulp tissue dissolution by passive ultrasonic irrigation in simulated accessory canals: impact of canal location and angulation. Int Endod J. 2009;42:59-65.
46. Boutsioukis C, Verhaagen B, Versluis M, Kastrinakis E, Wesselink PR and van der Sluis LW. Evaluation of irrigant flow in the root canal using different needle types by an unsteady computational fluid dynamics model. J Endod. 2010;36:875-9.
47. Boutsioukis C, Gogos C, Verhaagen B, Versluis M, Kastrinakis E and Van der Sluis LW. The effect of root canal taper on the irrigant flow: evaluation using an unsteady Computational Fluid Dynamics model. Int Endod J. 2010;43:909-16.
48. Boutsioukis C, Gogos C, Verhaagen B, Versluis M, Kastrinakis E and Van der Sluis LW. The effect of apical preparation size on irrigant flow in root canals evaluated using an unsteady Computational Fluid Dynamics model. Int Endod J. 2010;43:874-81.
49. Koch JD, Jaramillo DE, DiVito E and Peters OA. Irrigant flow during photon-induced photoacoustic streaming (PIPS) using particle image velocimetry (PIV). Clin Oral Investig. 2016;20:381-6.
50. Sirtes G, Waltimo T, Schaetzle M and Zehnder M. The effects of temperature on sodium hypochlorite short-term stability, pulp dissolution capacity, and antimicrobial efficacy. J Endod. 2005;31:669-71.

51. Dunavant TR, Regan JD, Glickman GN, Solomon ES and Honeyman AL. Comparative evaluation of endodontic irrigants against Enterococcus faecalis biofilms. J Endod. 2006;32:527-31.
52. Chavez de Paz LE, Bergenholtz G and Svensater G. The effects of antimicrobials on endodontic biofilm bacteria. J Endod. 2010;36:70-7.
53. Bukhary S and Balto H. Antibacterial efficacy of octenisept, alexidine, chlorhexidine, and sodium hypochlorite against Enterococcus faecalis biofilms. J Endod. 2007;43:643-647.
54. Swimberghe RCD, De Clercq A, De Moor RJG and Meire MA. Efficacy of sonically, ultrasonically and laser-activated irrigation in removing a biofilm-mimicking hydrogel from an isthmus model. Int Endod J. 2019;52:515-523.
55. Aerssens J, Boonen S, Lowet G and Dequeker J. Interspecies differences in bone composition, density, and quality: potential implications for in vivo bone research. Endocrinology. 1998;139:663-70.
56. Fouad AF, Walton RE and Rittman BR. Induced periapical lesions in ferret canines: histologic and radiographic evaluation. Endod Dent Traumatol. 1992;8:56-62.
57. Ferreira FB, Campos Rabang HR, Pinheiro ET, Gade-Neto CR, Zaia AA, Ferraz CC, de Souza-Filho FJ and Gomes BP. Root canal microbiota of dogs' teeth with periapical lesions induced by two different methods. Oral Surg Oral Med Oral Pathol Oral Radiol Endod. 2006;102:564-70.
58. Shin JM, Luo T, Lee KH, Guerreiro D, Botero TM, McDonald NJ and Rickard AH. Deciphering endodontic microbial communities by next-generation sequencing. J Endod. 2018;44:1080-1087.
59. Klindworth A, Pruesse E, Schweer T, Peplies J, Quast C, Horn M and Glöckner FO. Evaluation of general 16S ribosomal RNA gene PCR primers for classical and next-generation sequencing-based diversity studies. Nucleic Acids Res. 2013;41:e1.
60. Qian W, Ma T, Ye M, Li Z, Liu Y and Hao P. Microbiota in the apical root canal system of tooth with apical periodontitis. BMC Genomics. 2019;20 Suppl 2:189.
61. Wang Z, Shen Y and Haapasalo M. Effectiveness of endodontic disinfecting solutions against young and old Enterococcus faecalis biofilms in dentin canals. J Endod. 2012;38:1376-9.
62. Lee SJ, Wu MK and Wesselink PR. The effectiveness of syringe irrigation and ultrasonics to remove debris from simulated irregularities within prepared root canal walls. Int Endod. 2004;37:672-8.
63. Caputa PE, Retsas A, Kuijk L, Chavez de Paz LE and Boutsioukis C. Ultrasonic irrigant activation during root canal treatment: a systematic review. J Endod. 2019;45:31-44 e13.
64. Gutarts R, Nusstein J, Reader A and Beck M. In vivo debridement efficacy of ultrasonic irrigation following hand-rotary instrumentation in human mandibular molars. J Endod. 2005;31:166-70.
65. Burleson A, Nusstein J, Reader A and Beck M. The in vivo evaluation of hand/rotary/ultrasound instrumentation in necrotic, human mandibular molars. J Endod. 2007;33:782-7.
66. Klyn SL, Kirkpatrick TC and Rutledge RE. In vitro comparisons of debris removal of the EndoActivator system, the F file, ultrasonic irrigation, and NaOCl irrigation alone after hand-rotary instrumentation in human mandibular molars. J Endod. 2010;36:1367-71.

67. Uroz-Torres D, Gonzalez-Rodriguez MP and Ferrer-Luque CM. Effectiveness of the EndoActivator system in removing the smear layer after root canal instrumentation. J Endod. 2010;36:308-11.
68. Mancini M, Cerroni L, Iorio L, Dall'Asta L and Cianconi L. FESEM evaluation of smear layer removal using different irrigant activation methods (EndoActivator, EndoVac, PUI and LAI). An in vitro study. Clin Oral Investig. 2018;22:993-9.
69. De Meyer S, Meire MA, Coenye T and De Moor RJ. Effect of laser-activated irrigation on biofilms in artificial root canals. Int Endod J. 2017; 50:472-479.

Figures

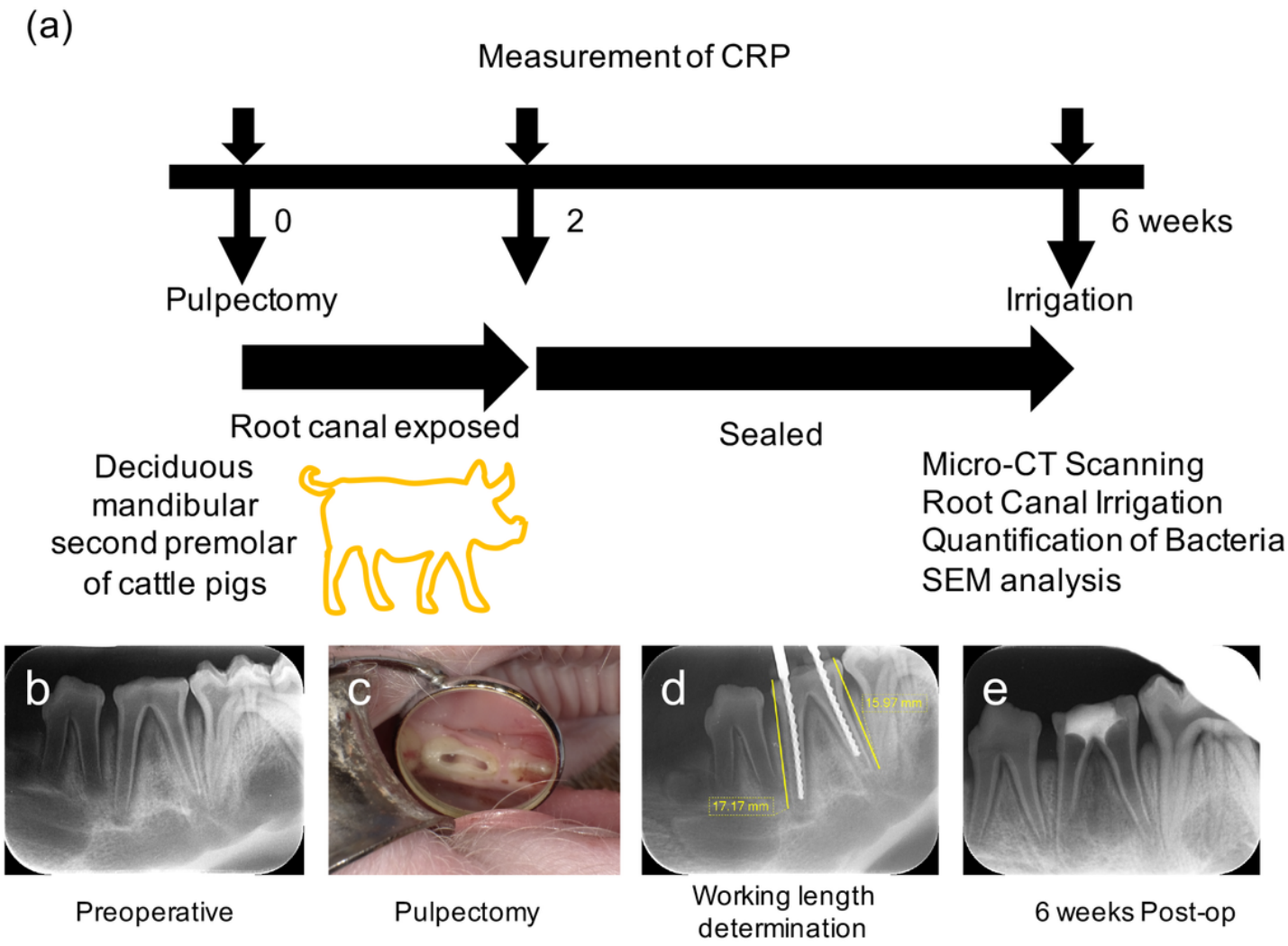

Figure 1

Experimental procedures for generating the intraradicular biofilm pig model. (a) CRP measurements were made at 0, 2, and 6 weeks after the pulpectomy to evaluate the inflammatory conditions in the pigs. Root canal irrigation was performed at 6 weeks. Micro-CT scanning, quantification of bacteria, and SEM analysis were performed to evaluate the periapical bone defect and intracanal infection. (b) Periapical

radiograph (PA) taken prior to the pulpectomy. (c) The access cavity was exposed to enable bacterial contamination from the oral environment. (d) Working lengths were determined from the PAs. (e) The access cavity was sealed with cement and composite resin at 2 weeks and maintained for a further 4 weeks.

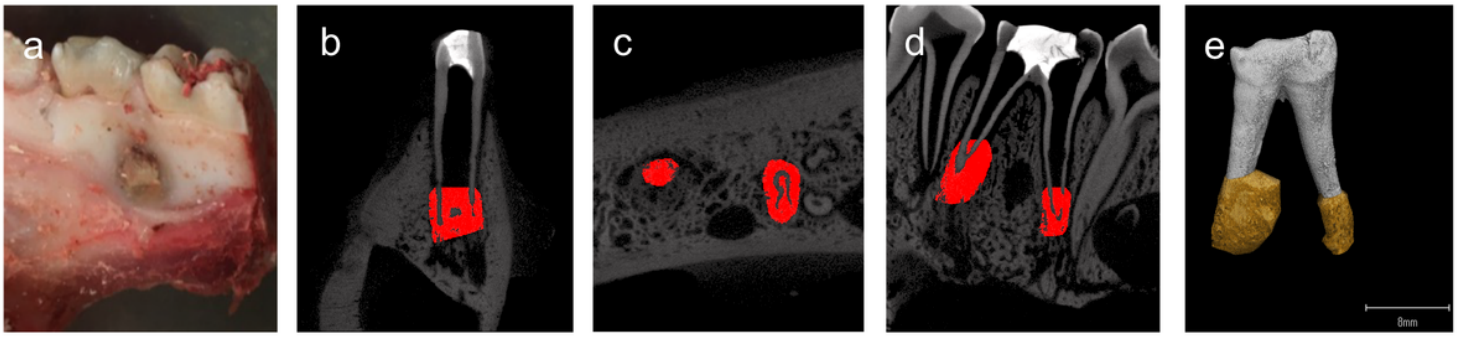

Figure 2

Analysis of the periapical lesions in the pig model. (a) Bone defect observed in a dissected mandibular jaw in the intraradicular biofilm pig model. (b) Frontal, (c) horizontal, and (d) sagittal views and (e) three-dimensional reconstruction of a treated tooth before extraction using micro CT scans.

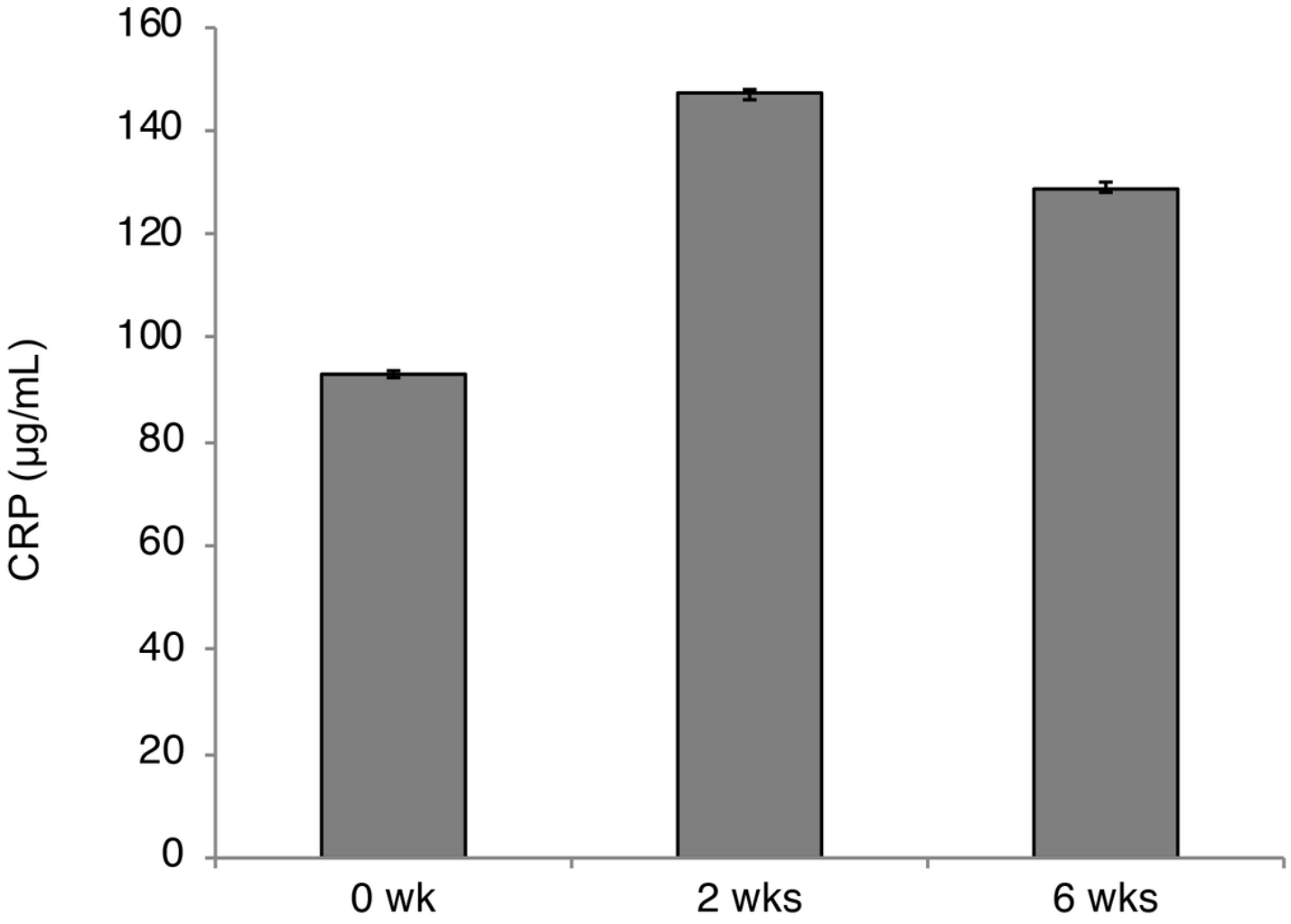

Figure 3

CRP measurements during periapical lesion formation. CRP measurements made at 0, 2, and 6 weeks after the pulpectomy in the pig model are shown on the graph. Data represent the means of three sample measurements; error bars indicate standard deviations.

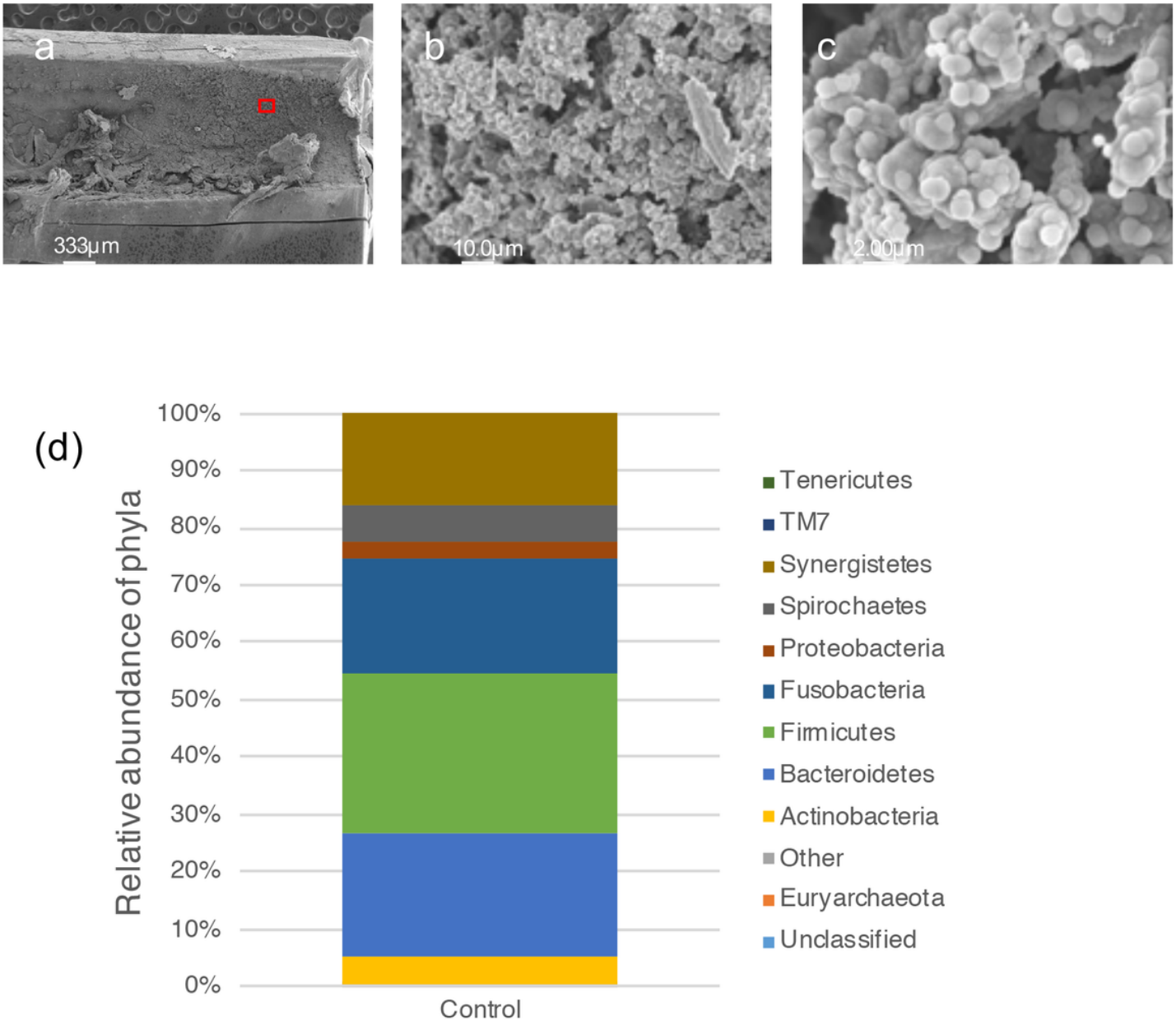

Figure 4

Morphological observations and bacterial 16S rRNA sequence analysis of the intraradicular biofilms in the pig model. SEM image of a root canal wall (30x) at the apical one third (a) and magnified views (1,000x and 5,000x) (b, c) of the boxed area are shown. (d) Relative abundance of bacterial phyla. Each color on the bar indicates a different phylum.

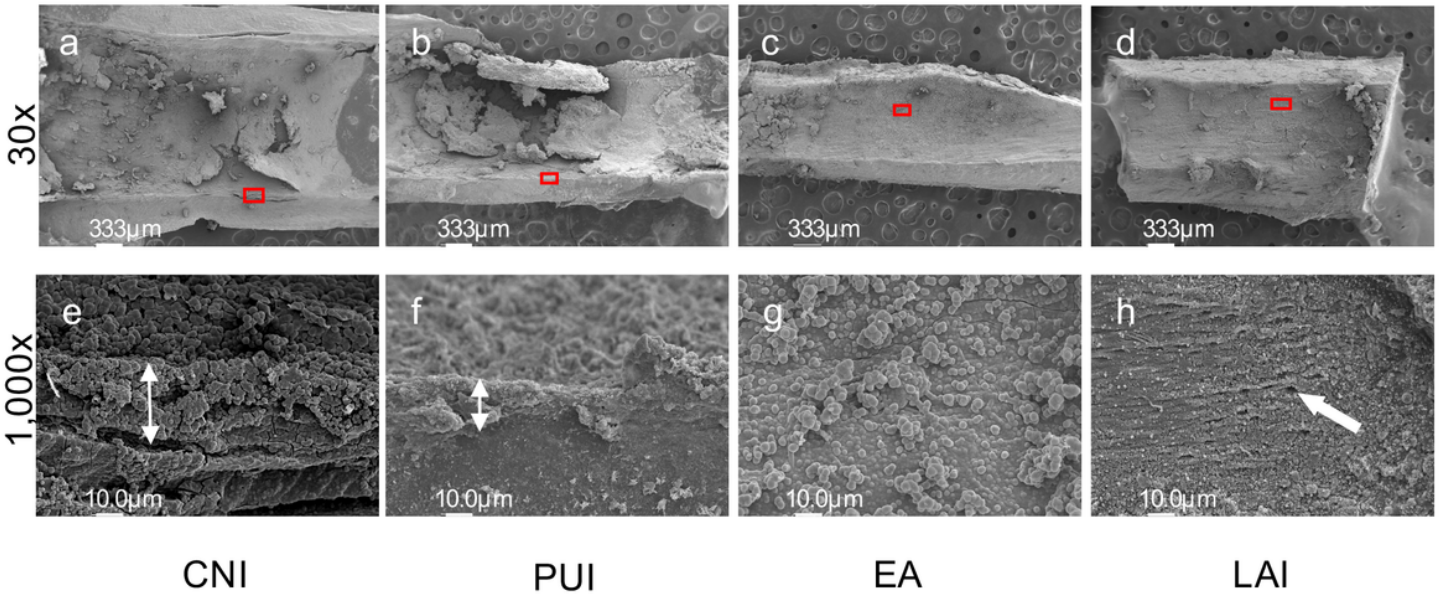

Figure 5

Morphological evaluations of each irrigation group. Effects of different root canal irrigation methods in the pig model including CNI (a, e), PUI (b, f), EA (c, g) and LAI (d, h) were investigated by SEM. (a-d) Images of the root canal wall at the apical one-third (30x). (e-h) Higher magnification views (1000x) of the red boxed areas are shown in the corresponding lower panel. (e, f) White double-headed arrows indicate the biofilm thickness. (h) White single-headed arrow denotes dentinal tubules.

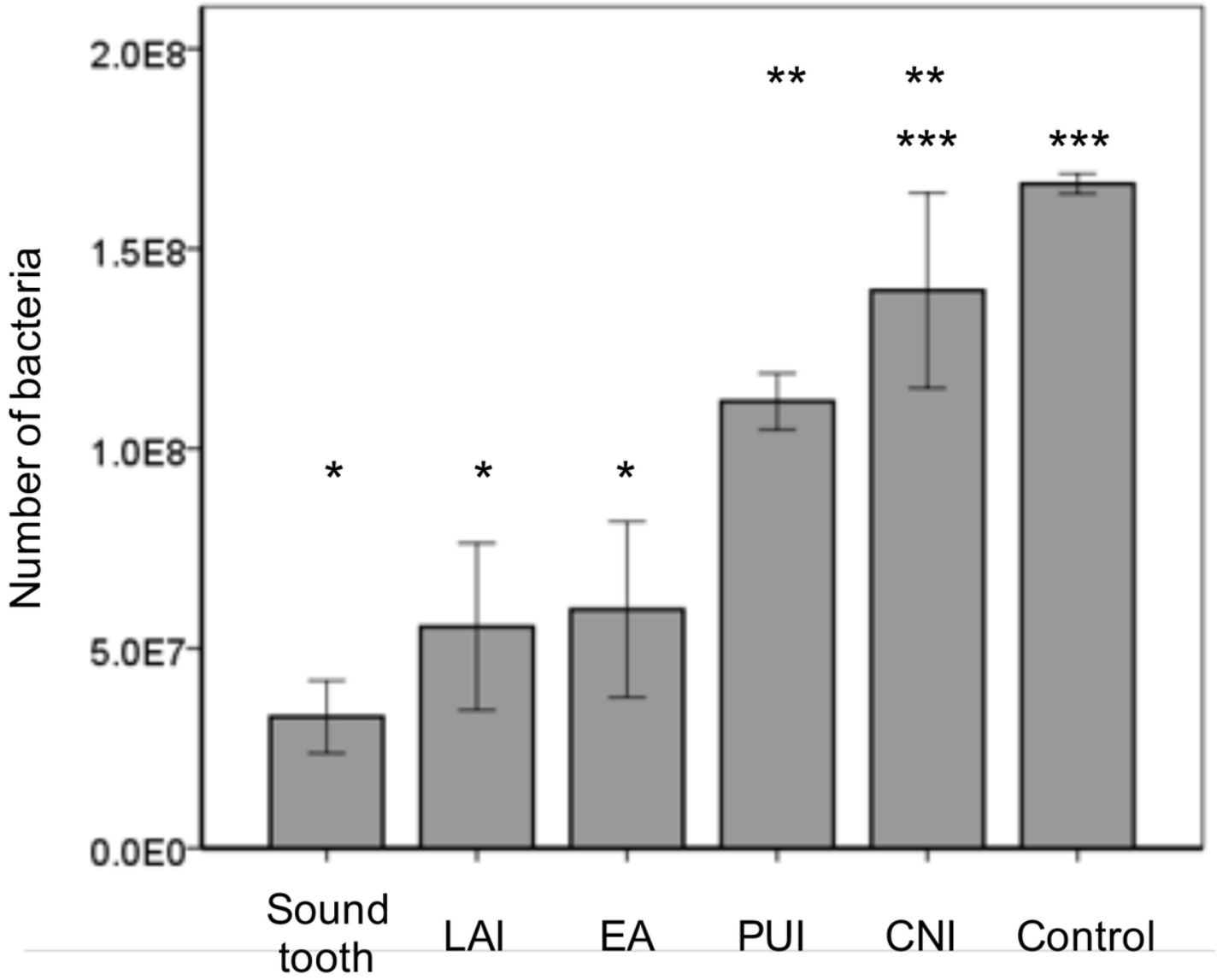

Figure 6

Quantitative analysis of each irrigation group. There were no significant differences between control and CNI, and CNI and PUI, among sound tooth, LAI and EA (Tukey Kramer test, $p<0.05$). The LAI and EA groups showed significant bacterial reduction compared with the PUI, CNI and Control groups (*).

Supplementary Files

This is a list of supplementary files associated with this preprint. Click to download.

- ARRIVEAuthorChecklistFull.pdf